Carnegie Observatories Astrophysics Series, Vol. 1:
Coevolution of Black Holes and Galaxies, 2004
ed. L. C. Ho (Pasadena: Carnegie Observatories,
http://www.ociw.edu/ociw/symposia/series/symposium1/proceedings.html)

AGN Black Hole Masses and Bulge Velocity Dispersions

R. F. GREEN[1], C. H. NELSON[2], and T. BOROSON[3]
(1) Kitt Peak National Observatory
(2) Drake University
(3) National Optical Astronomy Observatory

Abstract

Central black hole masses inferred from the reverberation mapping of emission lines from Active Galactic Nuclei fall on the same relationship with host bulge velocity dispersion as masses from stellar dynamical modeling. The velocity widths of both broad lines and forbidden lines may be used as moderate-scatter proxies for black hole mass determination in moderate luminosity AGNs. A preliminary examination of SDSS spectra of type-1 AGN shows a similar relationship between the broad-line proxy for black hole mass and the forbidden-line proxy for bulge velocity dispersion.

1.1 Reverberation Mapping

It is of fundamental interest to know how the masses of black holes in AGN relate to the masses of black holes in present-day quiescent nuclei. For distant hosts and/or luminous AGN, the glare of the nucleus inhibits direct measurement of stellar dynamics, even for the host bulge. Comparison of black hole mass determinations from emission-line properties of local AGN with the “gold standard" of the $M_{BH}-\sigma$ correlation gives hope for reasonable proxies for more distant objects.

As reviewed by Peterson (these Proceedings), reverberation mapping tracks the lag in response of a broad emission line to changes in the ionizing continuum flux. Such time monitoring allows the derivation of the radial distribution of Broad Line Region emitting clouds as a function of ionization potential of the species observed. The straightforward interpretation works for deriving the light travel time, τ_{LT}, because it is much smaller than the dynamical time of the BLR, on which the cloud geometry could change significantly. Since $\tau_{dyn} \sim r/\Delta v_{FWHM}$ and $\tau_{LT} \sim r/c$, $\tau_{dyn}/\tau_{LT} \sim c/\Delta v_{FWHM} \sim 100$. (Peterson 1997).

Peterson and collaborators (as summarized in Wandel, Peterson, & Malkan 1999) have conducted major campaigns of reverberation mapping. They have measured time lags for Hβ and UV broad lines of 2-20 days, dependent on the ionization potential. The interpretation is that the ionization is stratified, with "optimally emitting" clouds cooling most efficiently at the corresponding characteristic radius.

In principle, reverberation mapping can be used to estimate the black hole mass by measuring the velocity profile of only the variable component of the emission lines. The underlying physical assumption that must be verified is that the emitting regions that varied in response to changes in the ionizing continuum lie in close proximity to the ionizing source with velocity distributions dominated by orbital motion in the central gravitational potential.

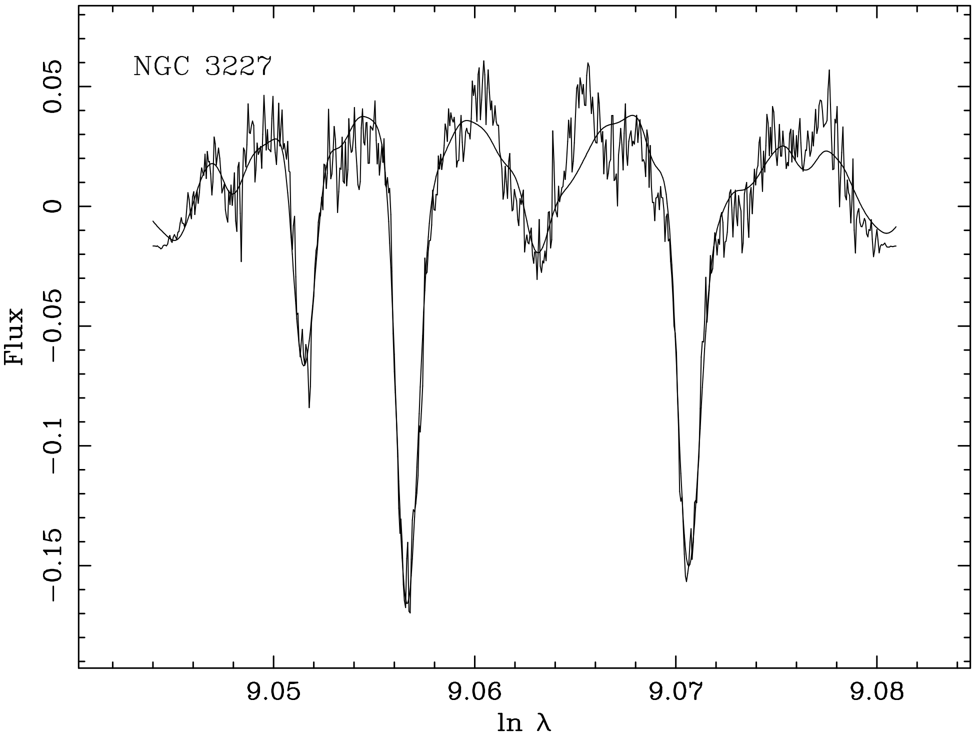

Fig. 1.1. Ca II triplet observation of NGC 3227, with the best parametric fit overplotted. A relatively early template star, F5 III, was required to match the strength of the Paschen line seen between the two stronger Ca II lines.

Then $M_{rev} = (1.45 \times 10^8\ M_\odot)\ (c\tau_{LT})v_{rms}^2$, where $c\tau_{LT}$ is in light days and v_{rms} is in units of $10^3 km/s$ (Peterson 1997). The assumption can be validated through a direct comparison with stellar dynamical black hole mass calibration in the same objects. In particular, the constant of proportionality will depend on detail on the types of motions of the BLR clouds in response to the gravitational potential.

1.2 Host Bulge Velocity Dispersions

The discovery of the tight relationship between central black hole mass and bulge stellar velocity dispersion (Gebhardt et al. 2000a, Ferrarese et al. & Merritt 2000) allows an independent test of the reverberation mapping results. Preliminary investigation by Gebhardt et al. 2000b showed no deviation from the normal galaxy relation for seven Seyfert 1 galaxies for which bulge velocity dispersions had been determined. Nelson (2000) used the profile of the [O III] line in place of direct stellar dynamical measurement for a somewhat larger sample, and found a similar result. (More on that topic below.)

C. Nelson, R. Green and their collaborators measured the bulge velocity dispersions of a sample of nearby reverberation-mapped Seyfert galaxies. They used the Kitt Peak National Observatory Mayall 4-meter telescope + RC Spectrograph. Attached to this heritage configuration was a new "red-hot" CCD from Lawrence Berkeley National Laboratories for its first science run on 10-14 April, 2001. That CCD is well matched to the task of measuring the Ca

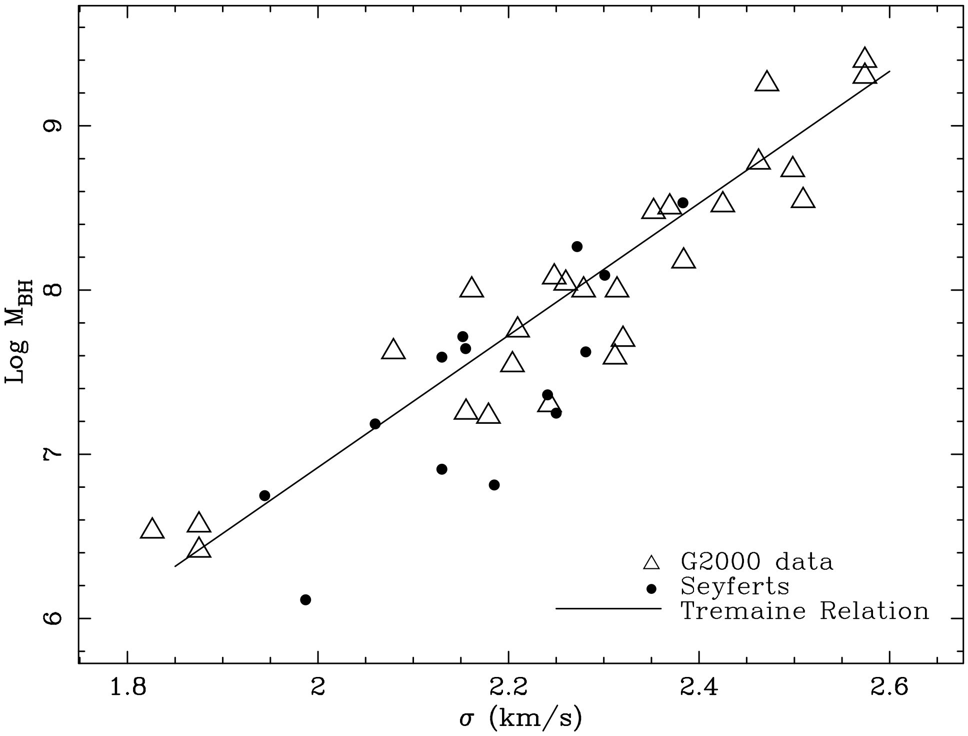

Fig. 1.2. Black Hole Masses Determined from Stellar Dynamics and Reverberation Mapping vs. Bulge Velocity Dispersion. The solid line is the relationship for stellar dynamical determinations fit by Tremaine et al. (2002).

II triplet feature for stellar dynamics. It has ∼90% DQE at 9000 Å and exhibits no fringing near that wavelength. A. Dey and R. Lynds led the project to adapt the nod-and-shuffle technique of K. Glazebrook (2001), which permitted excellent sky emission-line cancellation. Further reduction challenges included removal of contamination of the host galaxy stellar spectrum by the PSF wings of the AGN, and correction for telluric absorption. A sample spectrum is shown in Fig. 1.1.

Ensemble stellar motions can be described by the Line of Sight Velocity Distribution (LOSVD), which was fit parametrically with Gauss-Hermite polynomials to yield the moments. The LOSVD was derived from template matching through the Fourier Correlation Quotient method (Bender 1990). The far-red Ca II triplet feature near 8600 Å provides a robust template that is not very sensitive to modest reddening, dominant stellar spectral type, or metallicity.

The sample of objects observed was selected from the list of reverberation-mapped AGN from Wandel et al. (1999). The new data include 3C 390.3, Akn 120, Mrk 79, Mrk 110, Mrk 279, Mrk 590, Mrk 817, NGC 3227, NGC 4051, NGC 4151, NGC 4593, NGC 5548, and NGC 7469.

Fig. 1.2 shows that black hole masses inferred from reverberation mapping and from stellar dynamics correlate in a nearly identical relationship with bulge stellar velocity dispersion. We assume that systematic, three-integral modeling of the stellar dynamical data gives a reasonably accurate estimate of the central black hole mass. In that case, the tight agreement in the correlations validates the strong assumptions underlying the reverberation mapping technique:

- Line cooling from a given species lies in a relatively restricted zone at a definable effective distance from the nucleus.
- The motions of the emission line gas are dominated by response to the gravitational potential.
- The cross-correlation derivation of time lag of response of emission-flux to continuum variation is unambiguous.

Ferrarese et al. (2001) undertook a very similar investigation with substantial overlap in the samples. Initial comparison of the bulge stellar velocity dispersions for six objects in common showed the values of Nelson et al. to be 20-30 km/s higher. Nelson et al. used a 1" slit, compared to the 2" slit used by Ferrarese et al. The narrower slit may have excluded more of the cold disk contribution to the integrated spectrum.

1.3 Photoionization Modeling

It's worth remembering that the instantaneous measure of the width of the full broad-line profile can serve as an approximation to the rms width derived from reverberation mapping (Wandel, Peterson, and Malkan, 1999). The photoionization method assumes that the zone of line emission for each species in the BLR is located in a thin shell at a fixed distance from the central source. That distance in the physical source sets the ionization parameter, the one free parameter in the model that fits the line ratios. Wandel et al. showed that black hole masses derived from photoionization modeling and reverberation mapping agree with each other. The slope of the best-fit line differs from 1.0 by only 7%. That level of accuracy is consistent with the scatter of 8% internal to determinations for NGC 5548 over 6 observing seasons.

Given the success of the photoionization model, it is tempting to extend empirical calibration of velocity widths of other species against stellar dynamical black hole mass determinations. C IV is known to respond to UV continuum changes in monitored objects. McLure & Jarvis (2002) have shown that Mg II widths, when measured carefully by removing the neighboring complex of Fe II emission, also correlate with black hole mass. These correlations can be used to estimate black hole masses from line widths for higher redshift objects, to calculate the black hole mass function and its changes with cosmic time. The limitation of this technique may be reached if line profiles for higher luminosity objects are dominated by motions that do not scale directly with black hole mass (e.g., Netzer 2003).

1.4 [O III] as Proxy for Bulge Velocity Dispersion

There is also a proxy for assigning a bulge velocity dispersion to the host galaxy and inferring the black hole mass. Nelson and Whittle (1996) showed that the velocity width of [O III] $\lambda\lambda 5007, 4959$ is dominated by gravitational motions in the (bulge of the) galaxy for lower luminosity AGNs. There can be a contribution from bulk or thermal motions from outflow or shocks, but it does not dominate. The estimates obtained through this technique also agree with the stellar dynamical estimates of black hole mass, with even lower scatter than the broad-line values. Nelson (2000) demonstrated the effect for a sample of reverberation-mapped AGN.

Boroson (2002) is extending the comparison of the broad and narrow-line proxies to

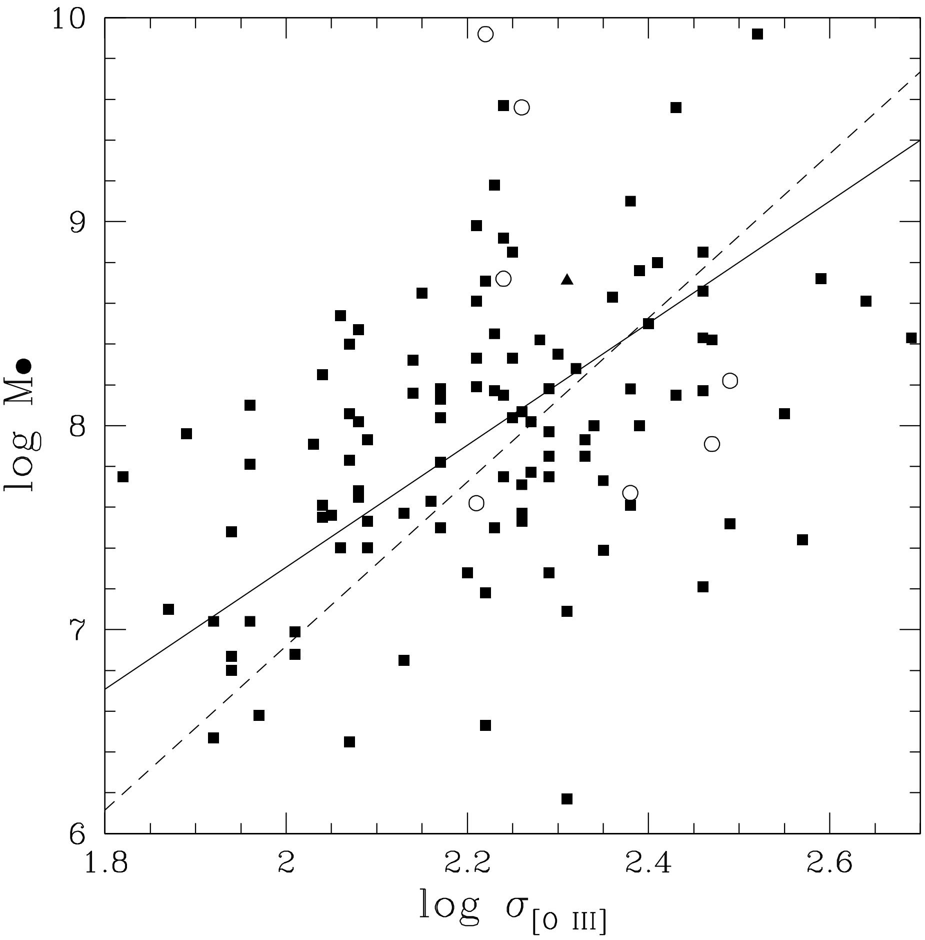

Fig. 1.3. Black hole mass, as calculated from Hβ FWHM and L, vs. σ from [O III]. Radio-loud objects are open circles, radio-quiet are squares, and the single radio-unobserved object is a triangle. The solid line is a least-squares bisector fit and the dashed line is the slope from Tremaine et al. for normal galaxies.

higher redshift. This work extends the initial investigation of Shields et al. (2002). He isolated a sample of 107 broad-line AGN with $z < 0.5$ from the SDSS early-release data and measured their Hβ and [O III] widths after modeling and subtracting the distributed Fe II emission. The photoionization model assumption for the combination of luminosity plus broad Hβ velocity width serves as the proxy for black hole mass. Figure 1.3 shows that value plotted against bulge velocity dispersion as inferred from σ for the [O III] lines. The dispersion in log BH mass is 0.67. The correlation coefficient is $r = 0.44$, which corresponds to a probability of random association of $\sim 6 \times 10^6$. It is intriguing that the residuals seem to correlate with Eigenvector 1 (Boroson and Green 1992). At a fixed apparent black hole mass, points with discrepantly higher "bulge dispersions" have narrower Hβ lines, higher luminosity, smaller [O III]/Hβ central intensity ratios, and larger Fe II equivalent widths, and the opposite is true for residuals to lower [O III] velocity width.

Wandel (1999) and Ho (1999) found that inferred black hole masses are 3-5 times smaller in AGN than in normal galaxies, based on the bulge luminosity-black hole mass relation. Estimates for bulge luminosities for the sample of reverberation mapped Seyfert galaxies are presented by Nelson (these Proceedings) and confirm the impression that they lie well off the normal galaxy correlation. Those galaxies do follow the $M_\bullet - \sigma$ relation for normal bulges, as shown above. Therefore, a more consistent interpretation is that the AGN host bulges are systematically more luminous than normal bulges. In that respect, it is interesting to note the requirement for an F-type template in Fig. 1.1, suggesting the presence of a younger stellar population in that object.

References

Bender, R. 1990, A&A, 229, 441
Boroson, T. 2003, ApJ, 585, 647
Boroson, T. A., & Green, R. F. 1992, ApJS, 80, 109
Ferrarese, L., & Merritt, D. 2000, ApJ, 539, L9
Ferrarese, L., Pogge, R. W., Peterson, B. M., Merritt, D., Wandel, A., & Joseph, C. L. 2001, ApJ, 555, L79
Gebhardt, K., et al. 2000a, ApJ, 539, L13
Gebhardt, K., et al. 2000b, ApJ, 543, L5
Glazebrook, K., & Bland-Hawthorn, J. 2001, PASP, 113, 197
Ho, L. C. 1999, in Observational Evidence for Black Holes in the Universe, ed. S. K. Chakrabarti (Dordrecht: Kluwer), 153
McLure, R. J., & Jarvis, M. J. 2002, MNRAS, 337, 109
Nelson, C. 2000, ApJ, 544, L91
Nelson, C., & Whittle, M. 1996, ApJ, 465, 96
Netzer, H. 2003, ApJ, 583, L5
Peterson, B. M. 1997, An Introduction to Active Galactic Nuclei, (Cambridge: Cambridge Univ. Press)
Shields, G. A., Gebhardt, K., Salviander, S., Wills, B. J., Xie, B., Brotherton, M. S., Yuan, J., & Dietrich, M. 2003, ApJ, 583, 124
Tremaine, S., et al. 2002, ApJ, 574, 740
Wandel, A. 1999, ApJ, 519, L39
Wandel, A. 2002, ApJ, 565, 762
Wandel, A., Peterson, B., & Malkan, M. 1999, ApJ, 526, 579